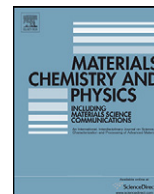




Contents lists available at ScienceDirect

## Materials Chemistry and Physics

journal homepage: [www.elsevier.com/locate/matchemphys](http://www.elsevier.com/locate/matchemphys)Preparation and characterization of sol–gel derived (Li,Ta,Sb) modified (K,Na)NbO<sub>3</sub> lead-free ferroelectric thin filmsLi Wang<sup>a</sup>, Ruzhong Zuo<sup>a,\*</sup>, Longdong Liu<sup>a</sup>, Hailin Su<sup>a</sup>, Min Shi<sup>a</sup>,  
Xiangcheng Chu<sup>b</sup>, Xiaohui Wang<sup>b</sup>, Longtu Li<sup>b</sup><sup>a</sup> Institute of Electro Ceramics & Devices, School of Materials Science and Engineering, Hefei University of Technology, Hefei 230009, PR China<sup>b</sup> State Key Lab of New Ceramics and Fine Processing, Department of Materials Science and Engineering, Tsinghua University, Beijing 100084, China

## ARTICLE INFO

## Article history:

Received 29 January 2011

Received in revised form 26 May 2011

Accepted 15 June 2011

## Keywords:

Thin films

Sol–gel growth

Ferroelectricity

Microstructure

## ABSTRACT

Lead-free ferroelectric thin film with a composition of  $(K_{0.4425}Na_{0.52}Li_{0.0375})(Nb_{0.8825}Sb_{0.08}Ta_{0.0375})O_3$  (KNLNST) has been successfully prepared on Pt/Ti/SiO<sub>2</sub>/Si substrate using sol–gel and spin-coating method. Polycrystalline perovskite films were obtained through pyrolysis at 400 °C and subsequent calcination at 700–800 °C for 30 min, which were optimized by means of X-ray diffraction and thermal analysis. The morphology on the top surface and fractured cross section of KNLNST films was observed by an atomic force microscope and a field-emission scanning electron microscope. Raman spectrum indicated that the film is almost stress-free as the film is thicker than 150 nm. The 300 nm-thick KNLNST film annealed at 750 °C exhibited a dielectric permittivity of 341, a loss tangent of 0.05 (1 kHz), a remanent polarization of 9.5 μC cm<sup>-2</sup> and a coercive field of 31.8 kV cm<sup>-1</sup>, as compared to the remanent polarization of 25.6 μC cm<sup>-2</sup> and the coercive field of 10 kV cm<sup>-1</sup> for bulk ceramics.

© 2011 Elsevier B.V. All rights reserved.

## 1. Introduction

Ferroelectric thin films have attracted great interest for a wide range of technological applications such as ferroelectric random access memory, micro-electro-mechanical system, pyroelectric infrared sensors, field effect transistor and so on. The most widely used ferroelectric film materials are based on Pb(Zr,Ti)O<sub>3</sub> due to their excellent piezoelectric and ferroelectric properties [1,2]. However, alternative lead-free ferroelectric films have attracted increasing attention in recent years owing to the Pb pollution, which involve Bi<sub>4</sub>Ti<sub>3</sub>O<sub>12</sub> [3], (Ba,Sr)TiO<sub>3</sub> [4], BaTiO<sub>3</sub>, (Bi,Na)TiO<sub>3</sub>-based [5] and (K,Na)NbO<sub>3</sub> (KNN) [6–15]. Among these lead-free ferroelectric films, KNN films have been considered as one of the most promising candidates for their relatively high Curie temperature, large piezoelectric longitudinal response  $d_{33}$  and high planar coupling coefficient  $k_p$  [8]. Many effects have been mostly focused on the effect of K and Na excess [9–11] or Li doping on the electrical properties of KNN films [12–15].

It is worthy noting that the ferroelectric properties of KNN films could be significantly improved by further optimizing their compositions. It has been reported that the (Li,Ta,Sb)-modified KNN ceramics exhibit excellent piezoelectric properties of  $d_{33} \sim 395$  pC N<sup>-1</sup> and  $k_p \sim 64\%$  [16,17]. Unfortunately, there

have been very few studies on KNN based films with such complex compositions, except that M. Abazari et al. reported the KNN–LiTaO<sub>3</sub>–LiSbO<sub>3</sub> films on SrTiO<sub>3</sub> substrate but fabricated by pulsed laser deposition (PLD) [18,19]. As known, the processing for making KNN ferroelectric films has been so far involved in various physical and chemical methods such as rf-magnetron sputtering [6,20,21], PLD [7,22], chemical solution deposition [12] and sol–gel processing [15,23,24]. Compared to other technologies, the sol–gel method has proved to offer advantages such as easiness of stoichiometry control, chemical homogeneity, low-temperature fabrication and reduced cost of equipment and so on, making it promising for producing homogeneous thin films. Unfortunately, this method has never been extended to the preparation of KNN based films with more complex compositions.

The purpose of this study is to deal with the fabrication and characterization of  $(K_{0.4425}Na_{0.52}Li_{0.0375})(Nb_{0.8825}Sb_{0.08}Ta_{0.0375})O_3$  (KNLNST) films deposited on Pt/Ti/SiO<sub>2</sub>/Si substrate using a conventional sol–gel method and spin-coating processing. The optimal processing conditions for preparing films were determined by using X-ray diffraction, thermal analysis, scanning electron microscopy and Raman spectroscopy. The effect of the annealing temperature on the microstructure, dielectric properties and ferroelectric properties of KNLNST films was studied in detail.

## 2. Experimental

Fig. 1 shows the flow chart for preparing the KNLNST sol via a conventional sol–gel process. Sb(CH<sub>3</sub>COO)<sub>3</sub> (≥99.9%), CH<sub>3</sub>COONa (≥99.0%), CH<sub>3</sub>COOK (≥92.0%),

\* Corresponding author. Tel.: +86 551 2905285; fax: +86 551 2905285.  
E-mail address: [piezolab@hfut.edu.cn](mailto:piezolab@hfut.edu.cn) (R. Zuo).

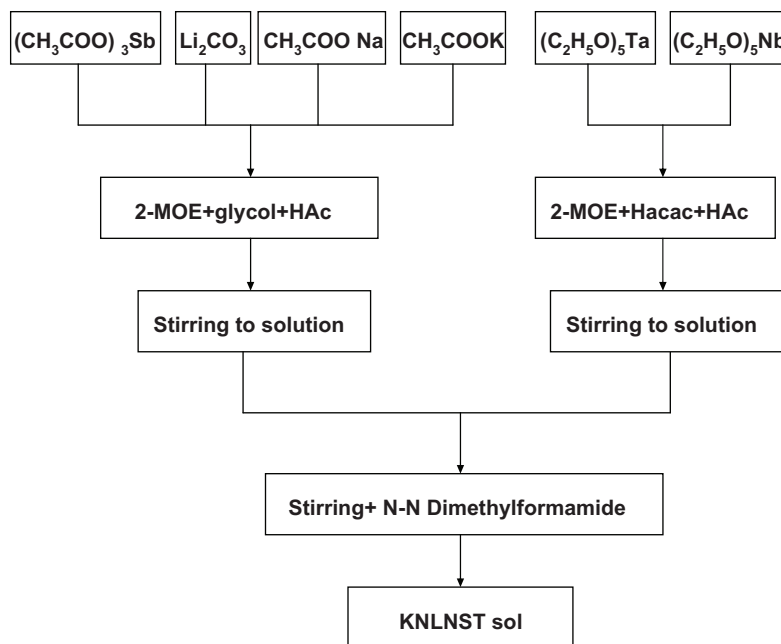


Fig. 1. Flow charts of preparing KNLNST sol via a sol-gel method.

$\text{Li}_2\text{CO}_3$  ( $\geq 99.0\%$ ),  $\text{Ta}(\text{OC}_2\text{H}_5)_5$  ( $\geq 99.95\%$ ) and  $\text{Nb}(\text{OC}_2\text{H}_5)_5$  ( $\geq 99.95\%$ ) were used as starting materials. According to the required stoichiometry,  $\text{Sb}(\text{CH}_3\text{COO})_3$ ,  $\text{Li}_2\text{CO}_3$ ,  $\text{CH}_3\text{COONa}$ , and  $\text{CH}_3\text{COOK}$  were dissolved in sequence in a solution containing 2-methoxyethanol (2-MOE), acetic acid (HAc) and 6 vol% glycol under continuous stirring at  $60^\circ\text{C}$ . Moreover, an appropriate portion of  $\text{Ta}(\text{OC}_2\text{H}_5)_5$  and  $\text{Nb}(\text{OC}_2\text{H}_5)_5$  was added to the 2-MOE solution, simultaneously with HAc and acetylacetone (Hacac) as the stabilizer and chelating agent, respectively. Subsequently, these two kinds of solutions were mixed and stirred to form a stable sol by adjusting the pH value to be  $\sim 5.4$ . N-N Dimethylformamide as drying control chemical additive was added into the sol precursor solution. 2-MOE was added to adjust the viscosity of the solution to obtain the concentration of 0.4 M. The KNLNST films were deposited on Pt/Ti/SiO<sub>2</sub>/Si substrates by a repeated spin-coating process with a spin rate of 3500 rpm for 30 s. After each spin-coating step, the films were dried at  $200^\circ\text{C}$  for 5 min and pre-annealed at  $400^\circ\text{C}$  for 8 min to remove organic components. Finally, the precursor films obtained by repeating the above-mentioned procedure were annealed in air at various temperatures from 700 to  $800^\circ\text{C}$  for 30 min in a tube furnace.

Thermo-gravimetry (TG) and differential scanning calorimetry (DSC) analysis of the dried KNLNST gel sample was carried out using a simultaneous thermal analyzer (STA409C, Netzsch, Germany). The phase composition and structure of KNLNST films annealed at different temperatures were characterized by an X-ray diffractometer (XRD, D/MAX2500 VL/PC, Rigaku, Japan). Raman spectra of the films were obtained by means of Raman spectrometer (LabRAM HR800, HJY, France). The morphology on the top surface and fractured cross section of the films was observed by an atomic force microscope (AFM, SPA-300HV Seiko, Japan), and a field-emission scanning electron microscope (FE-SEM, Sirion200, FEI, USA). Punctate Au electrodes with a diameter of  $150\ \mu\text{m}$  were deposited through a shadow mask on the films for electrical measurement. The polarization versus electric field ( $P$ - $E$ ) hysteresis loops were measured using a ferroelectric tester (Precision LC, Radiant Technologies, Inc., USA). The dielectric properties (permittivity and loss tangent) as a function of frequency were measured by an LCR meter (Agilent, 4980A, USA).

### 3. Results and discussion

#### 3.1. Thermal decomposition

The thermal decomposition behavior of the dried precursor gel is shown in Fig. 2. A weight loss of 3.1% at temperatures up to  $\sim 215^\circ\text{C}$  was assigned to the evaporation of organic solution. Two exothermic peaks at  $319^\circ\text{C}$  and  $407^\circ\text{C}$  could be attributed to the thermal decomposition of carboxylate-alkoxide precursors, corresponding to a weight loss of 18.2%. An exothermic peak at  $538^\circ\text{C}$  would be related to the combustion of residual organic components, accompanied by a weight loss of 3.5%. A step was found in the temperature range from 654 to  $780^\circ\text{C}$ , which was probably due to

the formation of a perovskite phase. From the results, a three-step heat treatment (low temperature drying at  $200^\circ\text{C}$ , pre-annealing temperature at  $400^\circ\text{C}$ , and annealing temperature ranging from 700 to  $800^\circ\text{C}$ ) could be tentatively identified.

#### 3.2. XRD spectra

Fig. 3 shows the XRD patterns of the KNLNST films annealed at various temperatures from 700 to  $800^\circ\text{C}$  for 30 min. It can be seen that all deposited KNLNST films started to be crystallized after annealing in the studied temperature range. The crystallization temperature range determined from XRD agreed well with the one estimated from TG-DSC curves (Fig. 2). Unfortunately, a few non-perovskite peaks were also observed and these peaks have been assigned to a secondary phase (indexed as  $\text{K}_2\text{Nb}_6\text{O}_{16}$ ). This is a compound devoid of potassium compared to the stoichiometry of KNLNST in which K/Nb is  $\sim 0.5$ . Therefore, the presence of this

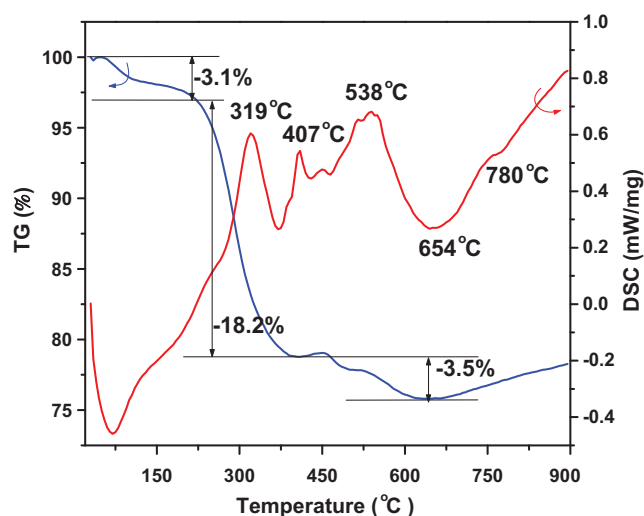


Fig. 2. Thermo-gravimetry and differential scanning calorimetry analysis of the KNLNST gel powders.

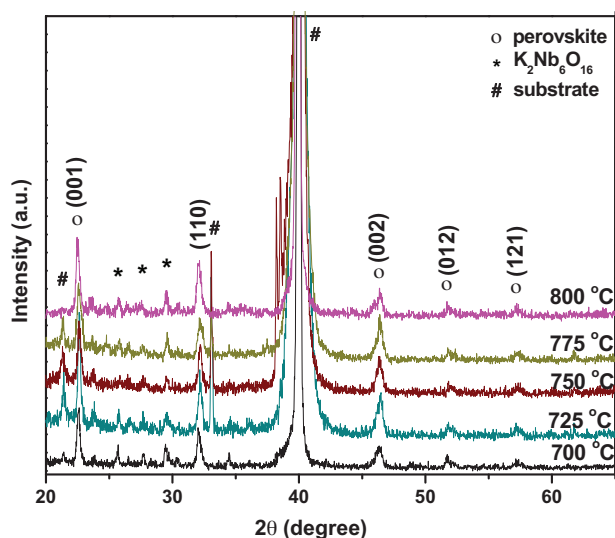


Fig. 3. XRD patterns of the KNLNST films annealed at different temperatures as indicated.

second phase may be due to the volatilization of K component. The intensity of the peaks assigned to  $K_2Nb_6O_{16}$  phase is relatively low at 750 °C. The annealing temperature of 750 °C was thus deemed to be the optimum temperature condition to ensure both better crystalline quality and less impurity phase.

### 3.3. Raman spectra

Raman spectra of KNLNST thin films with different thickness at room temperature are shown in Fig. 4. It can be found that the Raman spectra collected from the film samples annealed at 750 °C exhibit similar features to those of the ceramic powders of the same composition [25]. The peaks at around 245, 550 and 615  $cm^{-1}$  correspond to  $\nu_5$  ( $F_{2g}$ ),  $\nu_2$  ( $E_g$ ) and  $\nu_1$  ( $A_{1g}$ ) vibrational modes of  $NbO_6$  octahedra, respectively. The peak at around 860  $cm^{-1}$  is attributed to the combination mode of  $\nu_1$  ( $A_{1g}$ ) and  $\nu_5$  ( $F_{2g}$ ). All these indicate that the perovskite structure has been formed in the film as it was annealed at 750 °C. This is in good agreement with the XRD result (Fig. 3). In addition, tensile stresses usually arise within the

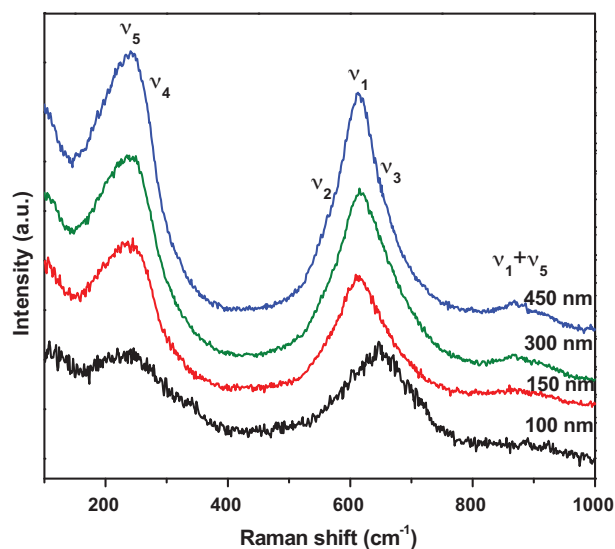


Fig. 4. Raman spectra of the KNLNST films with different thickness annealed at 750 °C.

films prepared by a solution-based method because of in-plane shrinkage of the film which is constrained by the substrate during heat treatment. The tensile stresses can be relieved by increasing the thickness of the films [26]. Huang et al. have ever made use of Raman spectroscopy to analyze the influence of the stress of films by the substrate [27]. It is worthy to note that the wavenumber of the  $\nu_1$  mode representing a double-degenerate symmetric O–Nb–O stretching vibration moves towards to higher value as the thickness of KNLNST film is lower than 100 nm. It could be considered that this stress is mainly caused by the mismatch of thermal expansion coefficients of the film and the substrate. When the thin film of KNLNST is thicker than 150 nm, the scattering position of the  $\nu_1$  mode is almost at the same position as that for the KNLNST powder [25], suggesting that films are almost stress-free. That is to say, the clamping effect by the substrate can be ignored in the film with the thickness of more than 150 nm. Similar Raman peak shift has been reported in  $(Pb,Ca)TO_3$  thin films by Mendiola et al. [28].

### 3.4. Morphology

The SEM micrograph on the cross-section of sol-gel derived KNLNST film annealed at 750 °C is shown in Fig. 5. It can be seen that the as-prepared film is homogeneous and dense, and sticks well to the substrate. The thickness of the film prepared by repeating spin-coating process for 6 times can be estimated to be  $\sim 300$  nm. No distinct interfaces could be observed between deposited layers. The top-surface morphology of the KNLNST film annealed at two different temperatures was examined by AFM, as shown in Fig. 6. It can be found that with increasing the annealing temperature, the film roughness was increased. A relatively smooth surface was observed for the film annealed at 750 °C, with a root-mean-square (rms) roughness value of 3.2 nm which is comparable to the value (rms=6.4) observed for 4% Li doped NKN films [13]. When the annealing temperature was raised to 800 °C, the roughness of the film was significantly increased (rms = 15.4) owing to the formation of pinholes. The possible reason could be ascribed to the volatilization of potassium component from the grain boundary of large grains or the formation of the second phase [29].

### 3.5. Dielectric and ferroelectric measurements

Frequency dependence of the permittivity and dielectric loss at room temperature for 300 nm-thick KNLNST films having under-

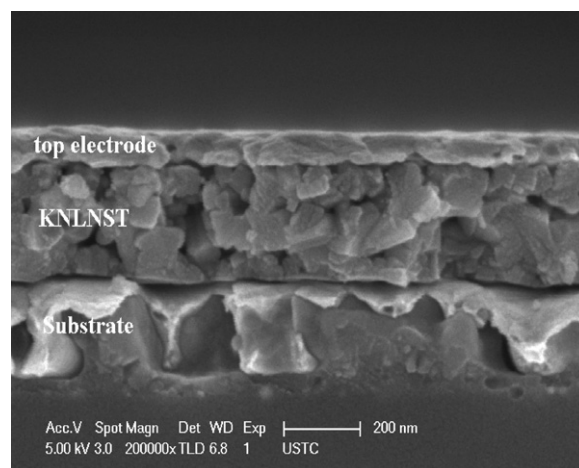


Fig. 5. SEM images on the cross section of the film annealed at 750 °C.

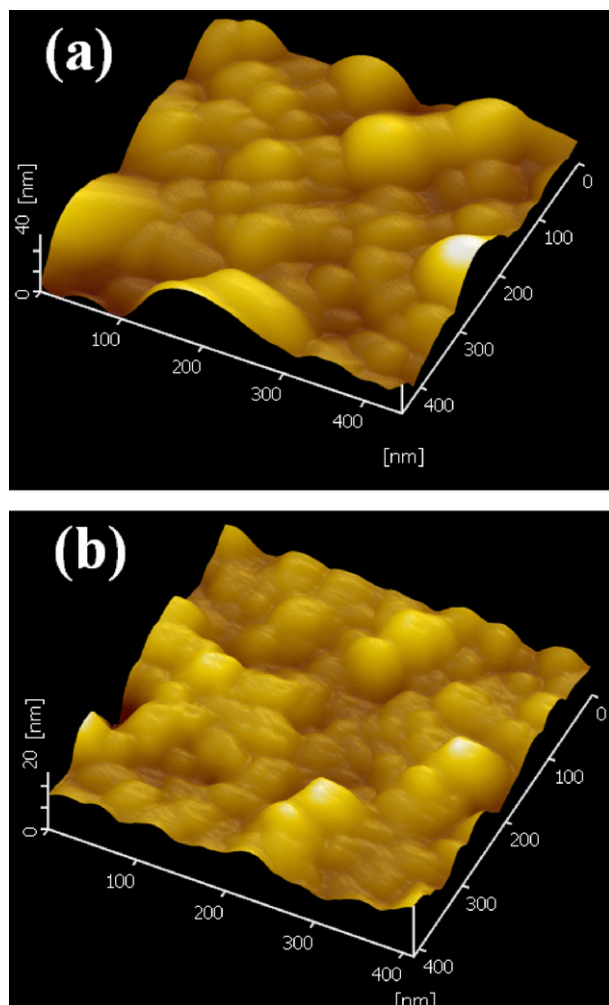


Fig. 6. AFM micrographs of the KNLNST films annealed at (a) 750 °C and (b) 800 °C.

gone different annealing conditions is shown in Fig. 7. A typical relaxation behavior was observed in the studied frequency range for all three films. The low-frequency dielectric relaxation could be attributed to the polarization of space charges in the film such as interfacial polarization of the Maxwell–Wagner type and the

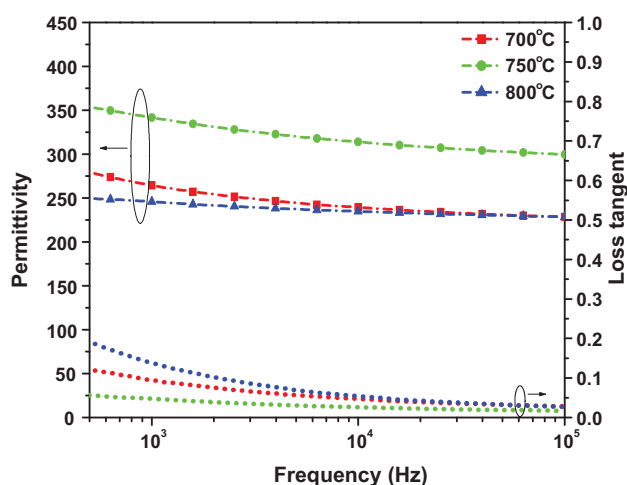


Fig. 7. Dielectric permittivity and loss tangent as a function of frequency for KNLNST films annealed at various temperatures.

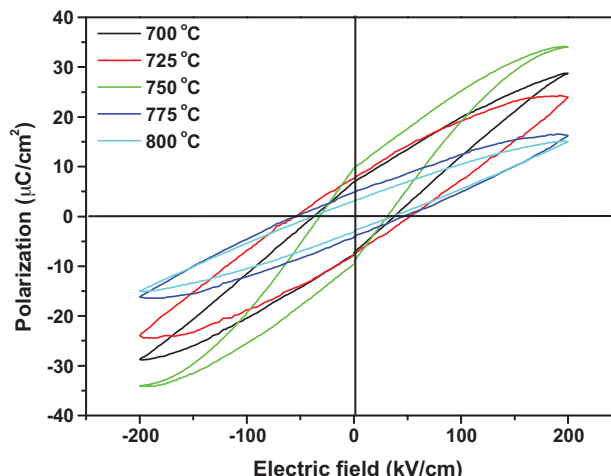


Fig. 8. *P*–*E* hysteresis loops of the KNLNST films on Pt/Ti/SiO<sub>2</sub>/Si substrates annealed at various temperatures for 30 min.

charged defects [30,31]. Meanwhile, the generation of charged defects may also originate from A-site vacancies and accompanying oxygen vacancies, which were formed by the volatilization of K during annealing. Furthermore, the film as annealed at 750 °C has higher dielectric permittivity (~341 at 1 kHz) and lower loss tangent (~0.05 at 1 kHz) than the other two films, indicating that the film annealed at 750 °C may possess lower defect concentrations at the film–substrate interface [32].

Fig. 8 shows the *P*–*E* hysteresis loops of 300 nm-thick KNLNST films annealed at various temperatures for 30 min. The loops were measured at a frequency of 2 kHz at room temperature. Higher electric fields could not be applied to the KNLNST film due to its low breakdown field. All films show typical ferroelectric behavior under an applied electric field of 200 kV cm<sup>-1</sup>. It can be seen that the remanent polarization (*P<sub>r</sub>*) of the films first increases as the annealing temperature increases from 700 to 750 °C and then decreases with further increasing the annealing temperature. A similar tendency with the annealing temperature was observed for the dielectric properties (Fig. 7). The KNLNST films annealed at 750 °C exhibit a typical *P*–*E* ferroelectric hysteresis loop with *P<sub>r</sub>* and coercive field (*E<sub>c</sub>*) of 9.5 μC cm<sup>-2</sup> and 31.8 kV cm<sup>-1</sup>, respectively, as compared to the *P<sub>r</sub>* value, 25.6 μC cm<sup>-2</sup> and the *E<sub>c</sub>* value, 10 kV cm<sup>-1</sup> of bulk ceramics [25]. The *P<sub>r</sub>* value is comparable to that of KNN-LT-LS film deposited by PLD [19]. However, KNLNST films annealed at 800 °C show relatively weak ferroelectricity (*P<sub>r</sub>* = 3.1 μC cm<sup>-2</sup> and *E<sub>c</sub>* = 38.9 kV cm<sup>-1</sup>). The possible reason can be given as follows: first, more non-perovskite K<sub>2</sub>Nb<sub>6</sub>O<sub>16</sub> phase appears in the film as annealed at 800 °C (Fig. 3); secondly, the evaporation loss of potassium component at higher annealing temperature tends to cause the presence of holes and a relatively low density as observed by AFM.

#### 4. Conclusions

Polycrystalline KNLNST films have been deposited on Pt/Ti/SiO<sub>2</sub>/Si substrate using sol-gel and spin-coating technique. The optimal pyrolysis and annealing temperatures were identified to be 400 °C and 750 °C, respectively. The SEM and AFM images indicated that the 300 nm-thick film annealed at 750 °C has relatively dense and uniform microstructure without cracks. The KNLNST film annealed at 750 °C exhibited good dielectric and ferroelectric properties with the dielectric permittivity ~341 and *P<sub>r</sub>* ~ 9.5 μC cm<sup>-2</sup>. The results indicated that a conventional sol-gel method was successfully extended to the preparation of KNN based films with complex compositions.

## Acknowledgements

This work was financially supported by a project of Natural Science Foundation of Anhui Province (090414179), by the Fundamental Research Funds for the Central Universities, and by the National Natural Science Foundation of China (50972035) and a Program for New Century Excellent Talents in University, State Education Ministry (NCET-08-0766) and 973 Program (No. 2009CB623301).

## References

- [1] A. Suárez-Gómez, J.M. Saniger-Blesa, F. Calderón-Piñar, *Mater. Chem. Phys.* 123 (2010) 304.
- [2] C.Q. Liu, W.L. Li, W.D. Fei, S.Q. Zhang, J.N. Wang, *J. Alloys Compd.* 493 (2010) 499.
- [3] J.H. Park, J.S. Bae, H.J. Park, Y.S. Kim, B.E. Jun, B.C. Choi, J.H. Jeong, *Thin Solid Films* 516 (2008) 5304.
- [4] J. Du, K.L. Choy, *Mater. Sci. Eng. C* 26 (2006) 1117.
- [5] Y.P. Guo, D. Akai, K. Sawada, M. Ishida, *Solid State Sci.* 10 (2008) 928.
- [6] J.G. Wu, J. Wang, *J. Appl. Phys.* 106 (2009) 066101.
- [7] C.R. Cho, A. Grishin, *Appl. Phys. Lett.* 75 (1999) 268.
- [8] F.P. Lai, J.F. Li, *J. Sol-Gel Sci. Technol.* 42 (2007) 287.
- [9] C.W. Ahn, S.Y. Lee, H.J. Lee, A. Ullah, J.S. Bae, E.D. Jeong, J.S. Choi, B.H. Park, I.W. Kim, *J. Phys. D: Appl. Phys.* 42 (2009) 215304.
- [10] K. Tanaka, H. Hayashi, K. Kakimoto, H. Ohsato, T. Iijima, *Jpn. J. Appl. Phys.* 46 (2007) 6964.
- [11] Y. Nakashima, W. Sakamoto, H. Maiwa, T. Shimura, T. Yogo, *Jpn. J. Appl. Phys.* 46 (2007) L311.
- [12] C.W. Ahn, E.D. Jeong, S.Y. Lee, H.J. Lee, S.H. Kang, I.W. Kim, *Appl. Phys. Lett.* 93 (2008) 212905.
- [13] F.P. Lai, J.F. Li, Z.X. Zhu, Y. Xu, *J. Appl. Phys.* 106 (2009) 064101.
- [14] N.T. Chua, L. You, J. Ma, J.L. Wang, *Thin Solid Films* 518 (2010) 6777.
- [15] K. Tanaka, K.I. Kakimoto, H. Ohsato, T. Iijima, *Ferroelectrics* 358 (2007) 175.
- [16] R.Z. Zuo, J. Fu, D.Y. Lv, *J. Am. Ceram. Soc.* 92 (2009) 283.
- [17] Y. Saito, H. Takao, T. Tani, T. Nonoyama, K. Takatori, T. Homma, T. Nagaya, M. Nakamura, *Nature* 432 (2004) 84.
- [18] M. Abazari, A. Safari, *J. Appl. Phys.* 105 (2009) 094101.
- [19] M. Abazari, T. Choi, S.W. Cheong, A. Safari, *J. Phys. D: Appl. Phys.* 43 (2010) 025405.
- [20] M. Blomqvist, S. Khartsev, A. Grishin, *Integr. Ferroelectr.* 80 (2006) 97.
- [21] S. Khartsev, A. Grishin, J. Andréasson, J.H. Koh, J.S. Song, *Integr. Ferroelectr.* 55 (2003) 769.
- [22] E. Cao, J.F. Hu, H.W. Qin, F. Ji, M.L. Zhao, M.H. Jiang, *J. Alloys Compd.* 509 (2011) 2914.
- [23] X. Yan, W. Ren, X.Q. Wu, P. Shi, X. Yao, *J. Alloys Compd.* 508 (2010) 129.
- [24] F. Söderlind, P.O. Käll, U. Helmersson, *J. Cryst. Growth* 281 (2005) 468.
- [25] H.Q. Wang, R.Z. Zuo, J. Fu, Y. Liu, *J. Alloys Compd.* 509 (2011) 936.
- [26] S.N. Song, J.W. Zhai, X. Yao, *Mater. Sci. Eng. B* 145 (2007) 28.
- [27] Y.Q. Huang, M.D. Liu, Z. Li, Y.K. Zeng, S.B. Liu, *Mater. Sci. Eng. B* 97 (2003) 111.
- [28] J. Mendiola, M.L. Calzada, P. Ramos, M.J. Martín, F. Agulló-Rueda, *Thin Solid Films* 315 (1998) 195.
- [29] K. Tanaka, K.I. Kakimoto, H. Ohsato, *J. Cryst. Growth* 294 (2006) 209.
- [30] P.C. Goh, K. Yao, *J. Am. Ceram. Soc.* 92 (2009) 1322.
- [31] J. Suchanicz, *Mater. Sci. Eng. B* 55 (1998) 114.
- [32] N.L. Amsei Júnior, A.Z. Simões, L.S. Cavalcante, F. Moura, E. Longo, J.A. Varela, *J. Alloys Compd.* 461 (2008) 326.